Proceedings of the
2001 European Control Conference,
Porto, Portugal, pp. 3522–3527

ROLLOVER AVOIDANCE FOR STEERABLE VEHICLES BY INVARIANCE CONTROL

Dirk Wollherr*, Jörg Mareczek°, Martin Buss*, Günther Schmidt°

* Control Systems Group
Technical University Berlin
Sekr. EN 11, Einsteinufer 17
D-10587 Berlin, Germany
fax: +49-30-314-21137
e-mail: Dirk.Wollherr@TU-Berlin.de
Martin.Buss@TU-Berlin.de
http://www.rs.tu-berlin.de

° Institute of Automatic Control Engineering
Technische Universität München

D-80290 München, Germany
fax: +49-89-289-28340
e-mail: Joerg.Mareczek@ieee.org
Guenther.Schmidt@ei.tum.de
http://www.lsr.ei.tum.de

Keywords: Nonlinear control, vehicle rollover avoidance, Invariance Control

Abstract

In this paper we address the problem of vehicle rollover avoidance control by applying the novel control method of *Invariance Control* which allows a nonlinear and non smooth controller design together with a formal proof of stability. The presented strategy leaves a maximum degree of freedom for steering to the driver. In addition a time-discrete rollover avoidance controller suitable for implementation is derived, which is both, robust and real-time computable. We validate the proposed approach by hardware-in-the-loop simulations of the nonlinear vehicle with a human driver in the loop, using a force feedback steering device.

1 Introduction

The fundamental task of a driver is to guide a road vehicle along a desired path. From a system theoretic point of view an experienced driver acts as a controller employing his/her knowledge of the vehicle dynamics. The overall system dynamics can be decomposed into controlled and internal dynamics. The controlled dynamics represent the direction and length of the velocity vector of the vehicle's centre of mass while the internal dynamics describe the roll-, yaw-, and pitch-motion. Roll and yaw motion may become unstable, resulting in tilting and skidding. Hence, following [1], a driver's task can be divided into the path following task and the task of keeping the internal dynamics stable, also known as the disturbance attenuation task.

Recently, these stability problems have frequently been discussed [2]. Considerable effort has been put into developing systems that assist the driver to avoid tilting or skidding. Two electronic driver assistants are the Anti-Blocking System (ABS) and the Electronic Stability Program (ESP) developed by the Bosch company. These systems have the effect of improving stability of the yaw dynamics by braking of single wheels; a side effect is an improvement of the stability of the roll dynamics. Stable roll dynamics means that the vehicle does not tilt. The so called *rollover avoidance* is subject of [3], where an additional actuator located at the joint between the load and the chassis is used to modify the roll angle, thus improving stability of the roll dynamics. Another method using a controller that reduces the steering angle chosen by the driver is suggested in [4]. In both approaches the controller design is based on a linearized one-track vehicle model extended by an additional mass to model roll motions [5]. Formal arguments for stability of the underlying nonlinear system of the vehicle are not presented.

Based on the novel control method of *Invariance Control* (IC) [6, 7, 8] we present a *rollover avoidance controller* (RAC), which guarantees stable roll dynamics and leaves a maximum degree of freedom of steering to the driver. Our control design approach can be applied to a large class of nonlinear, nonsmooth vehicle models.

The key idea is that a state space region is calculated such that in its interior stable roll dynamics are guaranteed. As long as the system state remains inside the region the driver has full steering autonomy. When the system state hits the boundary of the region the steering is switched to the Invariance Controller (thus overriding the steering commands of the driver) to keep the region positively invariant. Control is switched back to the driver when his/her steering input drives the system state back into the interior of the invariance region. Major advantages of this approach are: (i) guaranteed stable roll dynamics; (ii) nonlinear controller design for less conservative results; (iii) optimal steering assistance with maximum driver autonomy.

We present two different designs for RACs, both based on IC. The first one is continuous time, using an exact input output linearization technique. The second RAC is discrete time but features real-time computability and can be made robust with respect to bounded physical parameter perturbations. The proposed RAC method is validated by a real-time simulation with a human driver in the loop. As control input active steering is used; see [9] for a discussion that this has larger effect on the internal dynamics than selective braking of the wheels.

In Section 2 the structure of the vehicle model used for the RAC design is presented. Section 3 provides some background of IC and the derivation of a continuous time RAC, a discrete time RAC is discussed in Section 4. The proposed control is evaluated in Section 5 by real-time simulations of a vehicle with elevated centre of mass and a human driver in the loop.

2 Model

We consider a nonlinear vehicle model of the form

$$\begin{aligned}\dot{\boldsymbol{x}} &= \begin{bmatrix}\hat{\boldsymbol{f}}({}_d\boldsymbol{x}) + \hat{\boldsymbol{g}}({}_d\boldsymbol{x}, \xi_1) \\ \boldsymbol{L}(\boldsymbol{\xi})\end{bmatrix} + \begin{bmatrix}\boldsymbol{0} \\ \boldsymbol{T}(\boldsymbol{\xi})\end{bmatrix}\delta \\ &= \boldsymbol{f}(\boldsymbol{x}) + \boldsymbol{g}(\boldsymbol{\xi})\,\delta\,, \end{aligned} \tag{1}$$

where the overall system state $\boldsymbol{x} = [{}_d\boldsymbol{x}^T\ \boldsymbol{\xi}^T]^T$ is divided into the state ${}_d\boldsymbol{x} \in \mathbb{R}^{n-r}$ of the chassis dynamics and the state $\boldsymbol{\xi} = [\xi_i] \in \mathbb{R}^r$ of the normal form feedback linearized, controlled steering dynamics.

We understand the controlled steering dynamics as the dynamics between the steering input δ (which is usually the position of the steering wheel) and the steering angle δ^w of the front wheels. These dynamics are supposed to admit a global normal form feedback linearization with respect to an output function $\xi_1 = \delta^w$, resulting in the dynamics of the second row of (1) with $\boldsymbol{L} = [\xi_2\ \cdots\ \xi_r\ L_r(\boldsymbol{\xi})]^T, \boldsymbol{T} = [0\ \cdots\ 0\ T_r(\boldsymbol{\xi})]^T$ and the normal form parameters $T_r(\boldsymbol{\xi}) \neq 0$, $L_r(\boldsymbol{\xi})$[10].

The chassis dynamics (first row of (1)) are described by a drift vector field $\hat{\boldsymbol{f}}$ and a control input vector field $\hat{\boldsymbol{g}}$ which are assumed to be smooth except for a finite number of l state-space surfaces where only the continuity property $\hat{\boldsymbol{f}}, \hat{\boldsymbol{g}} \in \mathcal{C}^0$ is given. This allows e.g. to take into account non-differentiable physical effects like tire characteristics of road vehicles.

The control input δ is subject to a state dependend constraint

$$\mathcal{D}(\boldsymbol{\xi}) = \left\{\delta |\ \delta^{min}(\boldsymbol{\xi}) \leq \delta \leq \delta^{max}(\boldsymbol{\xi})\right\}, \tag{2}$$

arising from limited actuator torques of the controlled steering dynamics. In the following we have $\delta = \delta^{drv}$ if a human driver determines the control input and $\delta = \delta^{inv}$ in case the presented electronic driving assistant steers the vehicle.

For this model we consider tilting as the situation when either the right-hand side or the left-hand side wheels of the vehicle loose contact to the ground. A quantitative measure is given by the *rollover coefficient*

$$R({}_d\boldsymbol{x}, \xi_1) = \frac{F_{z,R} - F_{z,L}}{F_{z,R} + F_{z,L}} \tag{3}$$

depending on the states $({}_d\boldsymbol{x}, \xi_1 = \delta^w)$ only, where $F_{z,R}$, $F_{z,L}$ denotes the right, left contact force of the vehicle to the ground. The rollover coefficient ranges between $-1 < R < 1$ when both sides of the vehicle have contact to the ground. Take off of the left (right)-hand side yields $R = +1$ ($R = -1$). According to (3) a rollover coefficient $|R| > 1$ is not possible and does not physically make sense. Moreover for ease of presentation we consider only left-hand side takeoff, i.e. we are only interested in keeping $R < 1$ (rather than $|R| < 1$).

Assumption 1 *For all non-equilibrium points of* (1) *there exists* $\xi_1^* = \delta^{w*}$ *such that* $|R({}_d\boldsymbol{x}, \delta^{w*})| - 1 \leq 0$, *i.e. there exists a suitable steering input* δ^{w*} *such that the vehicle does not tilt.*

We call a vehicle with this property a *steerable vehicle*. Note that we did not use the expressions *controllable* or *accessible* as they stand for much stronger conditions in the nonlinear case.

3 Rollover avoidance controller

Since a RAC using the steering angle as the control input effects the vehicle path and thus decreases the steering autonomy of the human driver, we define optimal rollover avoidance as a strategy that assures both, *maximum driver autonomy* and *stable roll dynamics*.

Definition 1 *Invariance Region/ Maximum Autonomy Region. Let* $\mathcal{G} = \{({}_d\boldsymbol{x}, \xi_1)|\ |R({}_d\boldsymbol{x}, \xi_1)| - 1 \leq 0\}$ *be the set of points where all wheels have ground contact. The boundary of* $\mathcal{G}$ *is given by* $\partial\mathcal{G} = \{({}_d\boldsymbol{x}, \xi_1)|\ |R({}_d\boldsymbol{x}, \xi_1)| - 1 = 0\}$. *We define a state space region* $\hat{\mathcal{G}} \subseteq \mathcal{G}$ *to be a suitable invariance region if it can be controlled positively invariant by a RAC, overriding the driver's control input action. In addition we define a maximum autonomy region* $\hat{\mathcal{G}}^*$ *as the maximally expanded region* $\hat{\mathcal{G}}$.

From the definition of a suitable invariance region $\hat{\mathcal{G}}$ it follows that the roll dynamics are stable if the system state is kept positively invariant in the interior of $\hat{\mathcal{G}}$. We now derive the switching Invariance Controller which is a RAC if the underlying invariance region is $\hat{\mathcal{G}}$.

With a (possibly) discontinuous output function $h = R({}_d\boldsymbol{x}, \xi_1) - 1$ we can decompose (1) into

$$\dot{\boldsymbol{x}} = \boldsymbol{f}_i(\boldsymbol{x}) + \boldsymbol{g}_i(\boldsymbol{x})\delta \quad \text{for: } \boldsymbol{x} \in \mathcal{D}_i,\ i \in \{1, \ldots, l\} \tag{4}$$

$$h_i({}_d\boldsymbol{x}, \xi_1) = R_i({}_d\boldsymbol{x}, \xi_1) - 1\,, \tag{5}$$

where the $\boldsymbol{x}$-state-space is divided into a number of l regions $\mathcal{D}_i \in \mathbb{R}^n$, $i \in \{1, \ldots, l\}$ with the property that in the interior of each region (1) is smooth. Then we can find coordinate transformations $\boldsymbol{z} = \boldsymbol{\Gamma}(\boldsymbol{x})$ with $\Gamma_k(\boldsymbol{x}) = \mathrm{L}_{\boldsymbol{f}_i}^{k-1} h_i({}_d\boldsymbol{x}, \xi_1)$ and a feedback linearizing control law

$$\delta(u, \boldsymbol{z}) = \frac{u - b_i(\boldsymbol{z})}{a_i(\boldsymbol{z})}, \quad \boldsymbol{z} \in \mathcal{D}_i, \tag{6}$$

with $a_i(\boldsymbol{z}) \neq 0$ and $b_i(\boldsymbol{z})$ as the standard normal form feedback linearizing coefficients for the relative degree r system (4), (5) achieving locally valid normal form representations

$$\dot{\boldsymbol{z}} = \boldsymbol{A}\,\boldsymbol{z} + \boldsymbol{b}\,u, \quad \boldsymbol{z} \in \mathbb{R}^r \tag{7}$$

$$\text{with respect to: } u^{min}(\boldsymbol{z}) \leq u \leq u^{max}(\boldsymbol{z})\,, \tag{8}$$

with $(\boldsymbol{A}, \boldsymbol{b})$ in Brunovsky canonical form and u as a virtual control input. The region $\mathcal{G}$ is now represented in the simple form $\mathcal{G} = \{\boldsymbol{z}|\ z_1 \leq 0\}$. More details about the derivation of locally valid normal forms can be found in [11].

Furthermore, we assume that sliding does not occur along possibly non-differentiable surfaces of system (1) controlled by (6) since in this case a system model of order less than r results as can be shown by the method of equivalent-control.

Without proof – see e.g. [12] – and assuming that $\partial\Upsilon(\boldsymbol{z})/\partial z_r \neq 0\ \forall \boldsymbol{z} \in \partial\hat{\mathcal{G}}$ – i.e. no so-called escape points [7, 8] exist on the boundary $\partial\hat{\mathcal{G}}$ – we give the following invariance result:

Theorem 1 *A region $\hat{\mathcal{G}} = \{\boldsymbol{z}|\ \Upsilon(\boldsymbol{z}) \leq 0\}$ with its boundary $\partial\hat{\mathcal{G}} = \{\boldsymbol{z}|\ \Upsilon(\boldsymbol{z}) = 0\}$ is positively invariant iff $\dot{\Upsilon}(\boldsymbol{z}) \leq 0$ for all $\boldsymbol{z} \in \partial\hat{\mathcal{G}}$, where $\Upsilon(\boldsymbol{z})$ is smooth with 0 as a regular value.*

Thus, the problem of guaranteeing stable vehicle roll dynamics is transformed into the problem of keeping $z_1 \leq 0$. The necessary and sufficient invariance condition hence is given by means of the time derivative of Υ along the trajectory of (7) as

$$\dot{\Upsilon} = \frac{d\Upsilon(\boldsymbol{z})}{d\boldsymbol{z}}\left(\boldsymbol{A}\boldsymbol{z} + \boldsymbol{b}\,u\right) \leq 0 \quad \forall \boldsymbol{z} \in \partial\hat{\mathcal{G}}. \tag{9}$$

Solving (9) for the control variable yields the Invariance Control input $u = u^{inv}$ which keeps $\hat{\mathcal{G}}$ invariant.

In order to leave as much steering autonomy as possible with the driver, we only override the driver's input if: (i) the state hits the boundary $\partial\hat{\mathcal{G}}$ *and* (ii) δ^{drv} is such that the state would leave the invariance region. From this we obtain the structure of the RAC as

$$\delta = \begin{cases} \delta^{drv} & \text{for } \boldsymbol{z} \in \hat{\mathcal{G}} \setminus \partial\hat{\mathcal{G}} \\ \delta^{inv}(u^{inv}(\boldsymbol{z}), \boldsymbol{z}) & \text{for } \boldsymbol{z} \in \partial\hat{\mathcal{G}} \ \wedge\ \dot{\Upsilon}(\boldsymbol{z}, \delta^{drv}) > 0\,, \end{cases} \tag{10}$$

where the second part of the control law results from (6) with $u = u^{inv}(\boldsymbol{z})$ from the invariance condition (9). Replacing $\boldsymbol{z}$ by $\boldsymbol{\Gamma}(\boldsymbol{x})$ we obtain the structure as shown in Fig. 1. The `decision unit` detects when the system state hits $\partial\hat{\mathcal{G}}$ and switches according to (10) between the driver and the `calculation unit`.

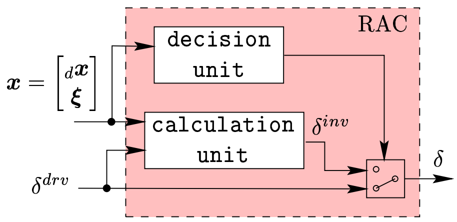

Figure 1: Structure of the RAC.

In the previous paragraphs we assumed a suitable invariance region $\hat{\mathcal{G}}$ to be given. Assuming the existence of constant control boundaries within the range of operation of the vehicle, i.e. $u^{\min} = \text{const}$, $u^{\max} = \text{const}$, one way to obtain such a region is to define its boundary by the switching surface of the time optimal control law for system (7)-(8). For the special case $r = 2$ the switching surface S of the time optimal control law has a qualitative form as shown in Fig. 2. Since the relation $z_1 = R - 1$ holds by the definition of the normal form coordinate transformation leading to system (7)-(8), we need to assure $z_1 \leq 0$ to prevent the vehicle from tilting. From this we can graphically derive a suitable invariance region $\hat{\mathcal{G}}$ as shown in Fig. 2. Hence, whenever the system state hits the upper part of the switching surface the maximum available control effort is

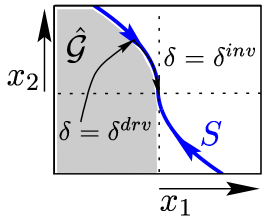

Figure 2: Suitable invariance region $\hat{\mathcal{G}}$ for $r = 2$.

applied ($u = u^{\min} \Rightarrow \delta = \delta^{inv}(u^{\min}, \boldsymbol{z})$) such that the system moves along $\partial\mathcal{G}$ into the origin.

In case the assumption of constant control boundaries is globally valid and not conservative, the switching surface S indeed represents the boundary of the maximum autonomy region $\hat{\mathcal{G}}^*$ since every other point above the upper part of S is not steerable back to $\hat{\mathcal{G}}$ without passing a region where $z_1 > 0$ holds. Hence, under this assumption there does not exist another region $\hat{\mathcal{G}}$ providing more steering-autonomy to the driver than the one shown in Fig. 2.

This idea of generating an invariance region $\hat{\mathcal{G}}$ can be extended to the case $r = 3$ as shown in detail in [11].

Summarizing the results of this section a four step design algorithm for a RAC can be formulated:

# 1	Calculate a globally valid output linearizing state feedback controller (6).
# 2	Find a conservative constant control limitation box for the linear system (7).
# 3	Compute the switching surface of a time optimal controller for the linear system (7) and determine the suitable invariance region $\hat{\mathcal{G}} = \{\boldsymbol{z} \mid \Upsilon(\boldsymbol{z}) \leq 0\}$.
# 4	RAC of Fig. 1: Calculate the invariance controller δ^{inv} from (6) and (9) for the invariance region $\hat{\mathcal{G}}$, serving as `calculation unit`. The `decision unit` follows from the evaluation of the invariance function Υ and its time derivative $\dot{\Upsilon}$ in the switching strategy (10).

4 Discrete Time RAC

Using a discrete time version of the RAC we omit the first two steps of the design algorithm; this results in a more conservative invariance region $\hat{\mathcal{G}}$. The discrete time version of a RAC is real-time computable and may provide a low cost implementation more appropriate for applications. The main difference to the preceding case is that the steering dynamics are now regarded as a perturbation to the system. To this purpose we approximate the steering dynamics by a pure time delay system $\delta^w(t + \tau) = \delta(t)$ with time delay $\tau > 0$.

Another difference arises from the fact that now $\mathcal{G}$ instead of $\hat{\mathcal{G}}$ is controlled invariant. Therefore the discrete time RAC obtains the steering autonomy when the system state has entered the region boundary layer $\mathcal{G} \setminus \hat{\mathcal{G}}$. The region $\hat{\mathcal{G}}$ is now defined by $\hat{\mathcal{G}} = \{({}_d\boldsymbol{x}, \xi_1)|\ \Upsilon({}_d\boldsymbol{x}, \xi_1) < -\varepsilon\}$ with $\Upsilon({}_d\boldsymbol{x}, \xi_1) = R({}_d\boldsymbol{x}, \xi_1) - 1$. The constant $\varepsilon > 0$ takes system perturbations into account such as the neglected steering dynamics, physical parameter perturbations and discrete time implementations.

As will be shown later, the size of ε increases as the perturbations grow. For a numerical calculation of the size of ε we model the perturbations which result from unprecisely known vehicle parameters by assuming a number of m physical vehicle parameters p_i with estimates $\hat{p}_i$. Following [6], we define an error vector $\boldsymbol{r} = [r_i] \in \mathcal{R}$ with relative errors $r_i = (p_i - \hat{p}_i)\,\hat{p}_i^{-1}$ and a bounded error space $\mathcal{R} = \{\boldsymbol{r} \mid |r_i| \leq \max(r_i), i \in \{1, \cdots, m\}\}$. Thus the chassis dynamics of (1) now depend on $\boldsymbol{r}$ also. Furthermore let $\mathcal{B} \in \mathbb{R}^{n-r}$ denote a closed set including the operational area of the state space of the chassis dynamics, determined by physical limitations of the chassis system states (such as e.g. maximum velocity). With these definitions we are able to determine a maximum rate of growth $\dot{R}^{\max}$ within the state space region $(\mathcal{G} \setminus \partial\hat{\mathcal{G}}) \cap \mathcal{B}$ by

$$\dot{R}^{\max} = \max \dot{R}({}_d\boldsymbol{x}, \delta, \boldsymbol{r}). \tag{11}$$
$$\text{with respect to } {}_d\boldsymbol{x} \in \left(\mathcal{G} \setminus \hat{\mathcal{G}}\right) \cap \mathcal{B}, \boldsymbol{r} \in \mathcal{R}, \delta \in \mathcal{D}(\boldsymbol{\xi})\,.$$

The value of $\dot{R}^{\max}$ is well defined as $\mathcal{B}$, $\mathcal{R}$, $\mathcal{D}$ are closed sets.

For a discrete time implementation we assume a constant sampling time Δt and the notation $\Upsilon_k = \Upsilon(k\,\Delta t), k \in \mathbb{N}_0$. Note that in the previous sections we always considered the *controlled* steering dynamics. Now, in order to formulate a discrete time RAC we have to do the following assumptions to the *underlying* controller:

Assumption 2 *Control of the steering dynamics.*
Consider the steering dynamics and a desired steering angle δ. The controller of the steering dynamics is such that there exists a time T^d with the property $\xi_1(t \geq T^d) \geq \delta$.

Without further loss of generality we may assume additionally $T^d = k\,\Delta t$. With this reasonable assumption to the steering dynamics we are able to formulate the following result for a discrete time RAC:

Theorem 2 *We consider a vehicle with the nonlinear chassis dynamics of the first row of (1) such that the corresponding rollover coefficient $R(t)$ is continuous. Moreover we assume the constant times Δt and T_d, a maximum variation of $\dot{R}^{\max}$ according to (11), and the resulting rollover security value*

$$\varepsilon = \dot{R}^{\max}(T^d + 2\,\Delta t). \tag{12}$$

to be given. Choosing the invariance angle δ^{inv} for all times t_k according to

$$\Upsilon({}_d\boldsymbol{x}, \delta_k^{inv}) = -\varepsilon, \quad \textit{for } ({}_d\boldsymbol{x}(t_k), \delta^w(t_k)) \in \mathcal{G} \setminus \hat{\mathcal{G}} \tag{13}$$

all wheels will have contact to the ground.

Remark to Theorem 2: Assume that the controller needs one sample period Δt to calculate and command a new control input δ, and a delay $\tau = T^d + \Delta t$ between the time when the state hits the boundary $\partial\hat{\mathcal{G}}$ and the time when the control input acts on the chassis. From (11) we know that during this time delay, the invariance function $\Upsilon(t)$ can maximally increase by $\dot{R}^{\max}\,\tau$. Clearly the discrete time controller cannot detect the exact time when the trajectory hits $\partial\hat{\mathcal{G}}$. Hence another delay Δt is needed such that $\varepsilon = \dot{R}^{\max}(T^d + 2\,\Delta t) = \dot{R}^{\max}(\tau + \Delta t)$.

Proof : of Theorem 2.
It will be shown that $\mathcal{G}$ is invariant, i.e. $\Upsilon < 0$ holds for all times. Therefore it is assumed that the trajectory leaves $\hat{\mathcal{G}}$ at time t^* within the interval $t_{k-1} \leq t^* < t_k$. The discrete time controller detects the state leaving $\hat{\mathcal{G}}$ after a time period less than Δt at the time t_k. With $\tau = T^d + \Delta t$ and (11) the invariance function $\Upsilon(t_k)$ can be estimated by

$$\begin{aligned}\Upsilon(t_k) &\leq \Upsilon(t^*) + \dot{R}^{\max}\Delta t = -\varepsilon + \dot{R}^{\max}\Delta t = \\ &-\dot{R}^{\max}(T_d + 2\Delta t) + \dot{R}^{\max}\Delta t = -\dot{R}^{\max}\tau.\end{aligned} \tag{14}$$

At time $t = t_k$ the invariance angle δ_k^{inv} is chosen according to Theorem 2 such that (13) holds. This has its impact – due to the time delay τ – at time $t_k + \tau$. During this period, i.e. for $t_k \leq t < t_k + \tau$, invariance of $\mathcal{G}$ is assured due to the choice of ε, since the inequality $\Upsilon(t) < \Upsilon(t_k) + \dot{R}^{\max}\tau = 0$ follows from (14). At time $t = t_k + \tau$ the invariance function evaluates due to $\delta^w(t+\tau) = \delta(t)$ to

$$\begin{aligned}\Upsilon(t_k + \tau)|_{\delta^w(t_k+\tau)=\delta_k^{inv}} &\leq \Upsilon(t_k)|_{\delta^w(t_k+\tau)=\delta_k^{inv}} + \\ &\dot{R}^{\max}\tau = -\varepsilon + \dot{R}^{\max}\tau = -\dot{R}^{\max}\Delta t\,.\end{aligned}$$

Inserting this result into the calculation of the following interval $t_k + \tau \leq t < t_{k+1} + \tau$, the invariance condition still holds:

$$\Upsilon(t, \delta_{k+1}^{inv}) < \Upsilon(t_k + \tau, \delta_k^{inv}) + \dot{R}^{\max}\Delta t \leq 0\,. \tag{15}$$

This proofs that for all $t \geq t^*$ where the Invariance Controller steers the vehicle, the invariance functionΥ is negative resulting in the postulated invariance of $\mathcal{G}$. ■

The structure of the RAC is equivalent to the continuous time case as shown in Fig. 1. However, instead of being determined by (10) the `decision unit` is now given by

$$\delta_k = \begin{cases}\delta_k^{drv} & \text{for } ({}_d\boldsymbol{x}_k, \xi_{1,k}) \in \hat{\mathcal{G}} \\ \delta_k^{inv} & \text{for } ({}_d\boldsymbol{x}_k, \xi_{1,k}) \in \mathcal{G} \setminus \hat{\mathcal{G}}.\end{cases} \tag{16}$$

Comparison: Discrete Versus Continuous Time RAC

Both RACs keep a suitable invariance region $\hat{\mathcal{G}}$ positively invariant. The `decision unit` detects in both cases the time when the state hits the boundary $\partial\hat{\mathcal{G}}$ in the continuous time case or $\mathcal{G}\setminus\hat{\mathcal{G}}$ in the discrete time case and switches δ^{drv} or δ^{inv} to the input of the steering dynamics. However, the `calculation unit` receives the value δ^{inv} from (13) in the discrete time and from (9) in the continuous time case.

In the continuous time case the region $\hat{\mathcal{G}}$ is determined without conservative assumptions; the price one has to pay is a high computational effort as this requires a state feedback linearizing control and in addition the computation of the switching surface of a time optimal controller.

In contrast to this, the region $\hat{\mathcal{G}}$ of the discrete time RAC is determined in a much simpler way by calculation $\dot{R}^{\max}$ and reducing $\mathcal{G}$ in a conservative way. Thus the main disadvantage is a reduced driver autonomy compared with the driver autonomy reached in the continuous time case.

5 Experiments

For real-time simulations the discrete time RAC was implemented to prevent a truck-like motor vehicle with an elevated center of mass from tilting. Therefore we used the well known nonlinear one-track model which is extended by an additional load to obtain a model that is able to perform roll motions.

The one-track model assumes a stiff chassis; the center of gravity CG_1 is located in the lane. As illustrated on the left of Fig. 3 the kinematics can be described by the speed vector $\boldsymbol{v}$, the angle β, and the yaw rate $\dot{\psi}$.

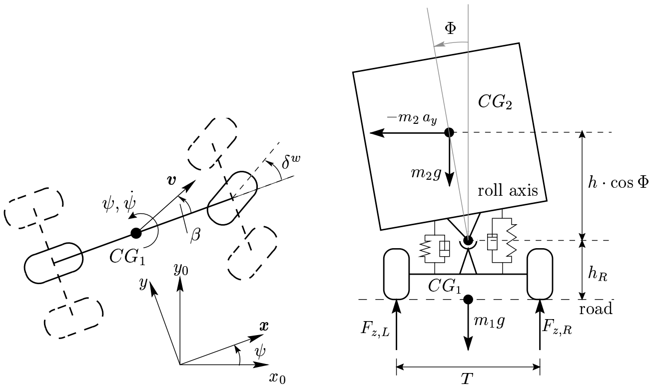

Figure 3: Top view of the one-track model and back view of the extended one-track model

This model features on the one hand simple equations of motion; on the other hand, it is not suitable for our purpose as it cannot perform roll motion. Following [5] an additional load mass is assumed to be mounted to the chassis through a spring-damper-system as shown on the right of Fig. 3. The center of gravity CG_2 of the second mass is located at a height h above the joint. The rolling angle of the second mass is denoted by Φ. With this extension, rolling and tilting is possible. Calculating the dynamics of the resulting extended one-track model yields a differential equation of the form of the first row of (1) where ${}_d\boldsymbol{x} = [\beta \; v \; \dot{\psi} \; \Phi \; \dot{\Phi}]^T$ is the state vector of the vehicle and the control input δ is the angle of the steering wheel. The model is nonlinear, especially as the function which is used to calculate the forces experienced by the tires, the HSRI tire model, has nonlinear, nonsmooth characteristics. The road is assumed to be flat and to have a constant adhesion coefficient everywhere, i.e. no μ-split. Loose or sloshing load is not considered, as discontinuous external forces make rollover avoidance impossible. The steering dynamics are of 3rd order with $\xi_1 = \delta^w$ as the steering angle on the wheels.

In order to test the discrete time RAC, a realtime simulator of the vehicle that allows to verify the functionality of the controller with a human driver in the loop is emplyed, i.e. the input does not follow a predetermined vehicle path so that the RAC has to cope with an unpredictable real driver's input.

5.1 Experimental Setup

The experimental setup is illustrated in Fig. 4. The block `vehicle` contains a real-time simulator based on (1) while the block `RAC` contains the discrete time RAC. Moreover the

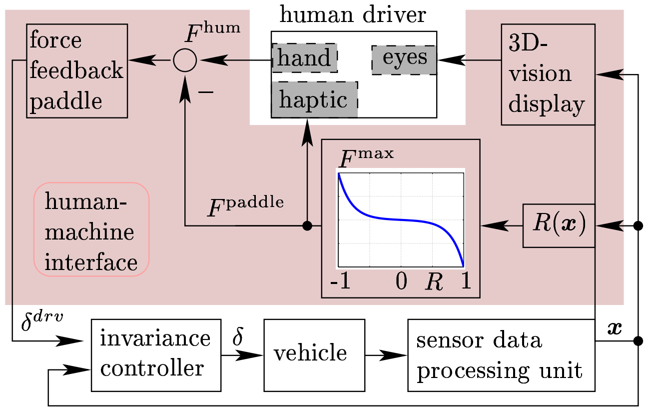

Figure 4: Simulation block diagram with a human in the loop.

human driver and the interface to the simulation existing of a force feedback steering paddle and a 3D-vision display is included. For a real system the system state ${}_d\boldsymbol{x}$ and δ^w must be estimated in an additional data processing unit as shown in Fig. 4.

Assuming a vehicle equipped with a steer-by-wire system implies that the driver does not necessarily feel forces on the steering wheel. If the driver gets no feedback on the controller status, shattering between the RAC and the driver might result if the driver – from a system theoretic point of view – does not have enough damping. The damping can be increased by interfacing the driver to the vehicle through a force feedback steering device using the force characteristic $F^{paddle}(t) = (e^{-\mu(R(t)+1)} - e^{-\mu(-R(t)+1)})F^{\max}$ with the maximum force F^{max} and $\mu = 10$.

In addition to the force feedback the driver receives visual information of the roll angle Φ by the horizon of the virtual driving scenario as well as the speed and direction (velocity vector $\boldsymbol{v}$) of the vehicle. Moreover, a bar changing its size proportionally to the size of R, and the position of a marking on the steering wheel indicate the status of the vertical forces to the ground.

5.2 Experimental Results

The driver is supposed to follow a straight two lane road. Pylons placed on alternating sides of the road force the driver to change lanes resulting in a slalom manoeuvre. The plots in Figs. 5 and 6 show a slalom manoeuvre performed by a human driver. The system parameters used for this simulation are identical to those used in [4], except for the bigger height $h = 1.8\,\mathrm{m}$ making the stabilization problem harder.

From Fig. 5 one can see that the driver tries to avoid three obstacles at a regular distance alternately blocking either lane of the road. Note that the scalings of the axes are different. The steering angle δ^{drv} corresponding to this manoeuvre is shown in the lower plot of Fig 6. In the experiment, $\varepsilon = 0.1$ in (13) was chosen. As soon as the rollover coefficient (see Fig. 6) exceeds the threshold of 0.9 (indicated by the dotted lines in the upper plot), the system switches to Invariance Control. The

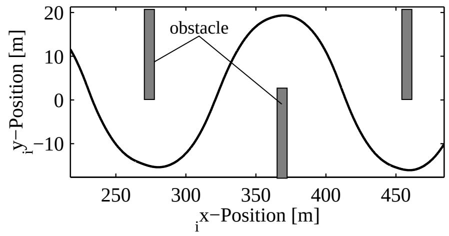

Figure 5: Driven trajectory avoiding three obstacles.

controller commands an angle δ^{inv} (dashed line in the lower plot) to the vehicle, which is smaller than the angle chosen by the driver.

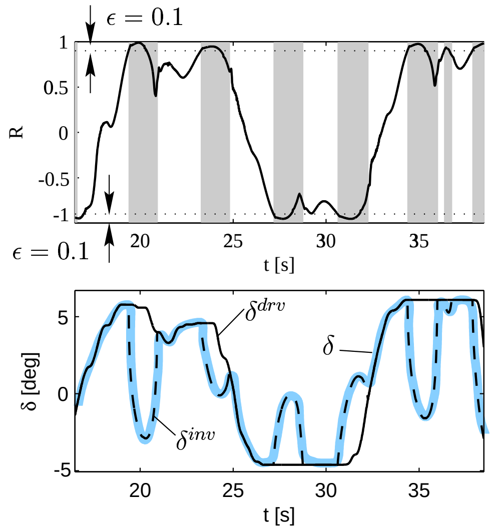

Figure 6: Plots of sample simulation results; solid/dashed line in the lower plot shows the steering angle δ^{drv} of the human driver and δ^{inv} of the RAC.

6 Conclusions and Outlook

Based on the novel nonlinear control method of *Invariance Control*, an approach for rollover avoidance of a general class of human driven vehicles was presented. Two RACs have been derived: the continuous time RAC provides high driver autonomy at the cost of high computational effort. The time-discrete RAC features real-time computability and robustness with respect to physical parameter perturbations. The disadvantage of the second controller is a slightly reduced driver autonomy compared to the continuous design.

The proposed approach is evaluated on a truck-like motor vehicle with an elevated center of mass in a real-time simulation with a human driver in the loop. The interface to the human driver includes a 3D-visual display of the road scenario and a force feedback steering device which is used to increase the damping of the human steering action and to provide a haptic interface to the roll dynamics.

Future work will include an extension of the continuous time RAC to steering dynamics of higher order. The presented RAC reduces only the lateral acceleration, resulting in a reduced radius of the driven vehicle path. This can be improved using the longitudinal acceleration as an additional control input for the RAC. Another important issue will be the enhancement of the interface to the human. Only an intuitive drive-by-wire haptic feedback will achieve enough driver confidence to delegate the steering autonomy to a control algorithm like the RAC.

Acknowledgments

The authors like to thank the members of the *multi-modal telepresence and teleaction research group* at TU München for their support during the development of the experimental setup and D. Odenthal for various useful comments. This work was supported in part by the German Research Foundation (DFG) within the Collaborative Research Center SFB 453 on *High-Fidelity Telepresence and Teleaction*.

References

[1] J. Ackermann, “Robust Control Prevents Car Skidding,” *IEEE Control Systems Magazine*, vol. 17, pp. 23–31, June 1997. 1

[2] A. T. van Zanten and R. Erhard and G. Pfaff, “VDC, The Vehicle Dynamics Control System of Bosch,” in *Advancements in ABS/TCS and Brake Technology (SP-1075)*, (Detroit, Michigan), pp. 9–26, 1995. 1

[3] R. C. Lin and D. Cebon and D. J. Cole, “Optimal roll control of a single-unit lorry,” in *Proc. IMechE*, vol. 210, part D, pp. 45–55, 1996. 1

[4] J. Ackermann and D. Odenthal, “Damping of Vehicle Roll Dynamics by Gain Scheduled Active Steering,” in *Proceedings of European Control Conference*, (Karlsruhe, Germany), 1999. 1, 5

[5] L. Segel, “Theoretical prediction and experimental substantiation of the response of the automobile to steering control,” in *Proc. IMechE*, pp. 310–330, 1956-1957. 1, 5

[6] J. Mareczek and M. Buss, “Robust Stabilization of SISO Non–Minimum Phase Nonlinear Systems,” in *Proceedings of the IEEE Conference on Decision and Control*, (Phoenix, AZ), pp. 2494–2595, 1999. 1, 4

[7] J. Mareczek, M. Buss, and G. Schmidt, “Invariance Control of Nonlinear Non–Minimum Phase Systems,” in *Proceedings of the 39th IEEE Conference on Decision and Control*, (Sydney, Australia), December 2000. 1, 3

[8] J. Mareczek and M. Buss, “Preliminary Studies on Geometric Invariance Control Synthesis,” in *Proceedings of European Control Conference*, (Karlsruhe, Germany, Paper No. 861), 1999. 1, 3

[9] J. Ackermann, T. Bünte, and D. Odenthal, “Advantages of active steering for vehicle dynamics control,” in *Proceedings of 32nd International Symposium on Automotive Technology and Automation*, (Vienna, Austria), pp. ME 263–270, 1999. 1

[10] A. Isidori, *Nonlinear Control Systems*. Berlin: Springer-Verlag, 3 ed., 1995. 2

[11] J. Mareczek, D. Wollherr, M. Buss, and G. Schmidt, “Rollover avoidance for steerable vehicles by invariance control,” Tech. Rep. TR1042001, Technical University Berlin, 2001. 2, 3

[12] H. Amann, *Ordinary differential equations*. Berlin, New York: Walter de Gruyter, 1990. 3